Bispecific designed ankyrin repeat proteins (DARPins) targeting epidermal growth factor receptor inhibit A431 cell proliferation and receptor recycling

Boersma, Y L ; Chao, G ; Steiner, D ; Wittrup, K D ; Plückthun, A

Abstract: The EGF receptor (EGFR) has been implicated in the development and progression of many tumors. Although monoclonal antibodies directed against EGFR have been approved for the treatment of cancer in combination with chemotherapy, there are limitations in their clinical efficacy, necessitating the search for robust targeting molecules that can be equipped with new effector functions or show a new mechanism of action. Designed ankyrin repeat proteins (DARPins) may provide the targeting component for such novel reagents. Previously, four DARPins were selected against EGFR with (sub)nanomolar affinity. As any targeting module should preferably be able to inhibit EGFR-mediated signaling, their effect on A431 cells overexpressing EGFR was examined: three of them were shown to inhibit proliferation by inducing G(1) arrest, as seen for the Food and Drug Administration-approved antibody cetuximab. To understand this inhibitory mechanism, we mapped the epitopes of the DARPins using yeast surface display. The epitopes for the biologically active DARPins overlapped with the EGF-binding site, whereas the fourth DARPin bound to a different domain, explaining the lack of a biological effect. To optimize the biological activity of the DARPins, we combined two DARPins binding to different epitopes with a flexible linker or with a leucine zipper, leading to a homodimer. The latter DARPin was able to reduce surface EGFR by inhibiting receptor recycling, leading to a dramatic decrease in cell viability. These results indicate that multispecific EGFR-specific DARPins are superior to cetuximab and may form the basis of new opportunities in tumor targeting and tumor therapy.

DOI: https://doi.org/10.1074/jbc.M111.293266

JBC Papers in Press. Published on October 6, 2011 as Manuscript M111.293266
The latest version is at http://www.jbc.org/cgi/doi/10.1074/jbc.M111.293266

Bispecific designed ankyrin repeat proteins (DARPins) targeting the epidermal growth factor receptor inhibit A431 cell proliferation and receptor recycling

Ykelien L. Boersma[1], Ginger Chao[2,3], Daniel Steiner[1,4], K. Dane Wittrup[2], and Andreas Plückthun[1*]

[1]From the Department of Biochemistry, University of Zurich, Winterthurerstrasse 190, 8057 Zurich, Switzerland

[2]The Department of Chemical Engineering and Bioengineering, Massachusetts Institute of Technology, 77 Massachusetts Avenue, Cambridge MA, 02139, USA.

[3]Present address: Adnexus, a Bristol-Myers Squibb R&D Company, 100 Beaver Street, Waltham MA, 02453, USA.

[4]Present address: Molecular Partners AG, Wagistrasse 14, 8952 Zurich-Schlieren, Switzerland

[*]Running title: *Bispecific EGFR-DARPins inhibit A431 cell proliferation*

To whom correspondence should be addressed: Andreas Plückthun, Department of Biochemistry, University of Zurich, Winterthurerstrasse 190, 8057 Zurich, Switzerland. Tel: +41-44-635 5570. Fax: +41-44-635 5712. Email: plueckthun@bioc.uzh.ch

Keywords: Designed ankyrin repeat proteins; EGFR; tumor targeting; protein engineering; epitope mapping.

Background: The EGF receptor is an important therapeutic target.
Results: Bispecific anti-EGFR-DARPins, alternative targeting molecules efficiently produced in bacteria, were shown to inhibit A431 cell proliferation and receptor recycling.
Conclusion: One bispecific construct containing four DARPins showed a biological activity superior to that of the registered antibody cetuximab.
Significance: Bispecific DARPins may form building blocks for tomorrow's cancer therapeutics.

SUMMARY

The epidermal growth factor receptor (EGFR) has been implicated in the development and progression of many tumors. While monoclonal antibodies directed against EGFR have been approved for the treatment of cancer in combination with chemotherapy, there are limitations in their clinical efficacy, necessitating the search for robust targeting molecules that can be equipped with new effector functions or show a new mechanism of action. Designed Ankyrin Repeat Proteins (DARPins) may provide the targeting component for such novel reagents. Previously, four DARPins were selected against EGFR with (sub)nanomolar affinity. As any targeting module should preferably be able to inhibit EGFR-mediated signaling, their effect on A431 cells overexpressing EGFR was examined: three of them were shown to inhibit proliferation by inducing G1-arrest, as seen for the FDA-approved antibody cetuximab. To understand this inhibitory mechanism, we mapped the epitopes of the DARPins using yeast surface display. The epitopes for the biologically active DARPins overlapped with the epidermal growth factor (EGF) binding site, whereas the fourth DARPin bound to a different domain, explaining the lack of a biological effect. To optimize the biological activity of the DARPins, we combined two DARPins binding to different epitopes with a flexible linker or with a leucine zipper, leading to a homodimer. The latter DARPin was able to reduce surface EGFR by inhibiting receptor recycling, leading to a dramatic decrease in cell viability. These results indicate that multispecific EGFR-specific DARPins are superior to cetuximab and may form the basis

of new opportunities in tumor targeting and tumor therapy.

The epidermal growth factor receptor (EGFR/ErbB1/HER1) was the first receptor identified of the ErbB family of receptor tyrosine kinases (1). These receptors, anchored in the cytoplasmic membrane, share a similar structure that is composed of an extracellular region containing a ligand-binding site, a transmembrane region, and a cytoplasmic tyrosine kinase domain (2, 3). The extracellular region itself is divided into four domains (I-IV). Domain I and III make direct contacts to the ligand, whereas domain II plays a role in receptor dimerization upon ligand binding (4). EGFR is known to bind a variety of ligands, including epidermal growth factor (EGF) and transforming growth factor-α (TGF-α) (5). These ligands can activate the receptor through inducing receptor dimerization, leading to transphosphorylation of key tyrosine residues. These residues provide specific docking sites for cytoplasmic proteins, whose binding initiates the signal for the activation of several downstream signaling pathways (6-8). Consequently, EGFR plays a pivotal role in cell proliferation and differentiation, and survival of normal epithelial tissue (9, 10). Signal attenuation is achieved by phosphatase activity. In addition, a ligand-induced alteration of EGFR trafficking leads to accelerated internalization of the receptor and a decrease in receptor recycling (11).

EGFR is constitutively expressed on many normal tissues, including the skin and hair follicles. The rationale for choosing EGFR as a target in cancer therapy was based on the observation that EGFR is overexpressed on the surface of many human cancers, including colorectal cancer, non-small cell cancer of the lung and gliomas (12). This overexpression is correlated with increased resistance to chemotherapy, more aggressive disease, and poor prognosis (6, 13). Moreover, increased receptor expression is often correlated with increased ligand production by the same tumor cells (1), leading to receptor activation by an autocrine stimulatory pathway. In some glioblastomas a mutant EGFR is expressed which contains a deletion in the extracellular domain, leading to a constitutively active receptor (14).

A number of monoclonal antibodies (mAbs) directed against EGFR have been extensively investigated for their abilities to slow or even inhibit tumor growth (15). FDA-approved antibodies cetuximab and panitumumab both bind to an epitope that partially overlaps the ligand-binding site of EGFR on domain III. Thus, the receptor is sterically prevented from adopting the open conformation required for dimerization. Consequently, autophosphorylation and receptor activation is inhibited (10, 16, 17). Nonetheless, the National Institute for Health and Clinical Excellence (NICE) for the U.K. (www.nice.org.uk) no longer recommends cetuximab in the treatment of metastatic colorectal cancer, based on an evaluation of an unfavorable ratio of clinical and cost effectiveness. The rather modest clinical benefits seen with cetuximab, an IgG, make molecular formats with novel effector functions, as well as novel multispecific formats with a new mechanism of action very desirable. In order to have an impact, such molecules must be easy to engineer and produce, and should be very robust to a wide range of modifications.

Several alternative binding scaffolds have been developed in recent years (18, 19), of which Designed Ankyrin Repeat Proteins (DARPins) are a particularly promising example (20). Derived from naturally occurring ankyrin repeat proteins, they have been engineered by a consensus design approach. DARPins have been selected from libraries via ribosome display or phage display to bind to a wide range of different protein targets (18, 21-26). DARPins are very well expressed in the cytoplasm of *Escherichia coli*, monomeric in solution, highly soluble and very stable; moreover, they can easily be fused to other protein domains to generate multispecific or multivalent DARPins, or be chemically conjugated to other molecules (27-29). Thus, the therapeutic application of DARPins can be extended over what would be possible with traditional antibodies.

Previously, four DARPins were selected by phage display against the soluble recombinant ectodomain of EGFR (21). These DARPins all showed monomeric behavior in size exclusion chromatography; additionally, their affinities were determined to be (sub)nanomolar (Table I). Using the A431 cell line, which has been developed as a widely used model system for testing anti-EGFR activity (30), we investigated the biological activity of these DARPins and compared them to that of cetuximab. Three DARPins were found to show biological activity on A431 cells, though their effect was not better

than the effect of cetuximab. The fourth DARPin did not show any biological activity.

Recently, it was established that combinations of noncompetitive mAbs can synergistically reduce surface EGFR levels, resulting in enhanced tumor cell killing (31, 32). To apply this principle to the selected DARPins, we first mapped the epitope of the four binders. We combined the non-competitive DARPins E01 and E69 in bispecific formats, using a flexible linker and a leucine zipper, respectively. Bivalent constructs with a flexible linker will be denoted as DARPin_GS_DARPin (to denote the $(G_4S)_2$ linker), whereas the leucine zipper constructs, which are both bispecific and bivalent and thus contain four DARPins, will be indicated by DARPin_LZx_DARPin. In particular, the E69_LZ3_E01 construct showed a dramatically improved biological activity compared to cetuximab. It could even reduce surface EGFR levels of A431 cells by inhibiting receptor recycling. These results indicate that bispecific DARPins hold great promise in tumor targeting strategies.

EXPERIMENTAL PROCEDURES

Cells and culture conditions – A431 cells were obtained from ATCC (ATCC number CRL-2592). Cells were maintained in DMEM culture media (Sigma, Steinheim, Germany) supplemented with 10% v/v heat-inactivated fetal calf serum (FCS, PAA GmbH, Pasching, Austria) and 1% v/v penicillin-G/streptomycin (Sigma) in a humidified incubator with 5% CO_2.

Reagents – Cetuximab was purchased from Merck (Darmstadt, Germany). Recombinant human epidermal growth factor (EGF) was purchased from Jena Bioscience GmbH (Jena, Germany). All chemicals used for overexpression and purification of the DARPins were purchased from Sigma-Aldrich, unless stated otherwise.

Cloning, expression and purification of DARPins – The ORFs for DARPins E01, E67, E68 and E69 recognizing EGFR and control DARPin Off7 were digested with *BamH*I and *Hin*dIII (Fermentas, Vilnius, Lithuania) and ligated into the expression vectors pQE30 and pQE30_sfGFP, the latter to create DARPins C-terminally fused to superfolder GFP (33). After transformation of *E. coli* XL-1 blue, the proteins were overexpressed, purified via their N-terminal $MRGSH_6$-tag with Ni-NTA superflow resin (Qiagen, Hilden, Germany), and subsequently dialyzed against PBS pH 7.2 (34).

Bispecific constructs of DARPins of E01 and E69 were made as described in (28). Briefly, the C-terminal DARPin was digested with *Bsa*I and *Bgl*II, and subsequently ligated into pQIBI vectors. The bispecific construct either had a flexible $(G_4S)_2$-linker between the two DARPins, or a leucine zipper; in the latter construct, the leucine zipper was both N-terminally and C-terminally flanked by different linkers (cf. Fig. 5A). The N-terminal DARPin was digested with *BamH*I and *Hind*III and ligated into the respective pQIBI vector. After transformation of *E. coli* XL-1 blue, the proteins were overexpressed, purified via their N-terminal $MRGSH_6$-tag, and subsequently dialyzed against PBS pH 7.2 (34).

DARPins E01 and E69_LZ3_E01 were coupled to Alexa Fluor 488 using maleimide chemistry. For this purpose, E01 was first subcloned into the vector pQE30_Cys after digestion with *BamH*I and *Hind*III. This vector has the sequence GSC appended to the C-terminus of the DARPin. In the E69_LZ3_E01 variant, the Cys residue present in the second repeat of E69 was first removed with the Quikchange kit (Stratagene, La Jolla, CA). Next, the C-terminal DARPin E01 was exchanged for E01_GSC after digestion with *Age*I and *Nhe*I and subsequent ligation. After transformation of *E. coli* XL-1 blue, the proteins were overexpressed and purified using the N-terminal $MRGSH_6$-tag. The proteins were dialyzed against HBS pH 7.5.

Binding of DARPin_sfGFP fusions to cells – A431 cells were trypsinized and resuspended in ice-cold FACS buffer (PBS pH 7.4, 1% BSA (Fluka), 0.1% sodium azide). For 1 hour, $1 \cdot 10^6$ cells were incubated with 100 nM of monovalent DARPin-sfGFP fusions on ice. As a positive control, cells were incubated with 100 nM cetuximab, which was subsequently labeled with an anti-human-Fab FITC-conjugated antibody (Jackson ImmunoResearch, Suffolk, UK). Off7_sfGFP and sfGFP itself were used as negative controls. The binding of the DARPins and cetuximab was examined using flow cytometry using a BD Biosciences FACSCantoII. Fluorescence data were analyzed using FlowJo software.

To determine the different epitopes of the DARPins, competition experiments were performed. One million cells were incubated with 50 nM of one DARPin-GFP fusion, with a series of concentrations of a second unlabeled DARPin or cetuximab as competitor. After a

1-hour incubation on ice, cells were washed twice with FACS buffer and the fluorescence was measured by flow cytometry.

Cell viability assays – For growth inhibition assays, A431 cells were seeded at a density of 3000 cells/well in DMEM supplemented with 1% v/v FCS. After 24 h, cells were treated with cetuximab or DARPins at different concentrations. Cells were incubated for another 72 h, after which cells were washed and incubated with 2,3-bis-(2-methoxy-4-nitro-5-sulfophenyl)-2H-tetrazolium-5-carboxanilide (XTT) (Roche) for 4 h at 37°C. Absorbance was measured at 540 nm in 96-well plates and expressed as a percentage of the untreated controls.

For clonogenic assays, A431 cells were seeded at a density of 300 cells/well in DMEM supplemented with 10% v/v FCS. After 2 h, 100 nM DARPin or cetuximab was added to the respective well. The treatment was terminated after 7 days: cells were washed twice with PBS and allowed to proliferate in DMEM supplemented with 10% v/v FCS for another 7 days. Cells were then stained with 0.1% crystal violet in PBS for at least 30 min at room temperature, after which colonies were counted. Clonogenic survival was expressed as the percentage of colony-forming units in treated cultures relative to untreated cultures (35, 36).

The concentration dependence of E69_LZ3_E01 was determined by the clonogenic assay as described above. Here, cells were treated with different concentrations, ranging from 10 pM to 1 µM. Cetuximab and Off7 were used as positive and negative controls, respectively.

Cell cycle analysis – A431 cells were seeded and plated onto 6-well plates at a density of $1 \cdot 10^6$ cells/well. Cells were maintained in DMEM, supplemented with 1% v/v FCS. After 24 h, cells were incubated alone or in the presence of 100 nM cetuximab or DARPin for another 24 h (37). Cells were permeabilized using 70% ethanol and cell cycle distribution was assessed by flow cytometry using propidium iodide staining (38). Single cells were gated and the resulting DNA distributions were analyzed using the FlowJo software.

Epitope mapping of DARPins – The epitopes of DARPins E01 and E69 were mapped according to the methods described in (39-41). Briefly, domain-level epitope mapping of E69 was performed by testing binding to yeast surface-displayed EGFR fragments. 10^6 yeast cells were incubated with 150 nM E69 for 30 min at 25°C, and subsequently labeled with biotinylated anti-penta-His antibody (1:100) (Qiagen) and streptavidin-PE (1:50) (Invitrogen) at 4°C. Fluorescence data were obtained using a Coulter Epics XL flow cytometer (Beckman-Coulter). Binding of E01 to yeast surface-displayed 404SG (see below) was performed in the same way.

Further fine epitope mapping (40) was performed using an error-prone PCR library of single point mutations of 404SG. 404SG is an EGFR ectodomain mutant carrying the point mutations A62T, L69H, F380S, and S418G, which allow the ectodomain to be correctly displayed on the surface of yeast (42). Misfolded 404SG EGFR variants were first removed through one round of FACS sorting for retention of binding to either 50 nM mAb 528 (binding to domain III) or mAb EGFR1 (binding to domain II) (Abcam, Cambridge MA, USA) (39, 40). Sorting was performed using either a DakoCytomation (Carpinteria, CA, USA), MoFlo or Aria (BD Biosciences) FACS machine at the MIT flow cytometry core facility. mAb 528 was shown not to compete with E01 for binding to EGFR (data not shown). Therefore, the mAb 528-positive library was sorted for loss of binding to E01 (sort 1 at 50 nM, sorts 2 and 3 at 100 nM DARPin). EGFR1 mAb had previously been shown not to compete with E69 for binding to EGFR (data not shown). Thus, the mAb EGFR1-positive library was sorted for loss of binding to E69 (sort 1 at 150 nM, sorts 2 and 3 at 300 nM E69). Plasmids from the enriched populations were recovered using a Zymoprep kit (Zymo Research, Irvine, CA, USA) and sequenced. Yeast was transformed with the individual sequenced mutants and re-tested to confirm proper folding of the EGFR mutants (by binding to the antibodies) and loss of binding to the DARPins.

All EGFR protein images were generated using PyMOL software (DeLano Scientific LLC, at http://www.pymol.org) from PDB structure 1IVO (chain A) (4).

Western blotting analysis – A431 cells were seeded and plated onto 6-well plates at a density of $1 \cdot 10^6$ cells/well. Cells were maintained in DMEM supplemented with 10% v/v FCS. After 24 h, the medium was changed to 1% v/v FCS for serum starvation in the presence of 100 nM cetuximab or DARPin for another 24 h. As a control, cells were incubated with serum starvation medium alone.

After this treatment, cells were stimulated with 10 ng/ml (1.6 nM) EGF for 15 min at 37°C and subsequently washed with PBS and incubated in lysis buffer (50 mM Tris pH 7.4, 150 mM NaCl, 0.5% w/v sodium deoxycholate, 0.1% v/v NP-40, 0.1% v/v SDS, 1 mM sodium orthovanadate, 1 tablet PhosStop (Roche)) (43-45). Total protein concentration in the lysates was determined by a BCA assay (Sigma) and 20 µg of total protein per sample was separated by 10% SDS-PAGE and transferred to an ImmobilonFL membrane (Merck Millipore, Billerica, MA, USA) by Western wet blotting. After blocking of the membranes with Odyssey blocking buffer (Li-Cor, Bad Homburg, Germany), the membranes were probed with the following antibodies from Cell Signaling Technologies (Beverly, MA, USA): α-phospho-EGFR (Tyr1068), α-EGFR, α-phospho-Akt (Ser473), α-Akt, α-phospho-ERK1/2 (phospho-p44/p42, Thr202/Tyr204), and α-ERK1/2. The anti-β-actin antibody was purchased from Sigma. After incubation with secondary IR-Dye-conjugated antibodies (Li-Cor), immunoblots were detected and quantified using the Odyssey software (Li-Cor).

Fluorophore labeling of DARPins – DARPins E01 and E69_LZ3_E01 were labeled with Alexa Fluor 488 C_5-maleimide (Molecular Probes, Invitrogen, Lucerne, Switzerland). DARPins were reduced under argon with 50 mM TCEP for 30 minutes. Then, TCEP was removed in a desalting step. DARPins were labeled with Alexa Fluor 488 at a protein:dye ratio of 3:1. The labeling reaction was allowed to proceed for 1 hour at room temperature. Unlabeled DARPins were separated from their labeled counterparts via anion exchange chromatography on a monoQ column using an NaCl gradient (50 mM Tris pH 8.5).

Internalization and recycling assays – The inhibition of receptor recycling was examined using the method described in (32). Briefly, A431 cells were serum starved for 16 h, after which they were harvested in serum-free medium. For 2 h, $2 \cdot 10^5$ cells were incubated with E01_Alexa Fluor 488 alone or in combination with E69, or with E69_LZ3_E01_Alexa Fluor 488 at 37°C to allow for internalization. Cells were then treated with 50 µg/ml anti-Alexa-488 quenching antibody (Invitrogen) for 30 minutes on ice and subsequently chased with unlabeled DARPin at 37°C for the indicated length of time in the presence of the quenching antibody. Cells were then returned to ice and washed twice with PBS. The subsequently measured fluorescence signal originated from the internalized labeled DARPins. The fluorescence signal was examined by flow cytometry using a BD Biosciences FACSCantoII. Fluorescence data were analyzed using FlowJo software; the percent unchased signal was calculated relative to cells that were not returned to 37°C after quenching. To verify the ability of E69_LZ3_E01 to inhibit receptor recycling, a monensin recycling assay was performed. A431 cells were serum starved for 16 h and subsequently harvested in serum-free medium to a concentration of $1 \cdot 10^6$ cells/ml. Cells were either treated with 50 µM monensin for 20 minutes at 37°C, or 100 nM E69_LZ3_E01. Incubation was continued at 37°C for the indicated time. Cells were then washed, acid stripped (0.2 M acetic acid, 0.5 M NaCl, pH 2.5), and washed again with PBS. Then, cells were incubated on ice with 100 nM E69_LZ3_E01_Alexa Fluor 488. After 45 minutes, cells were washed. The binding of the DARPin was analyzed by flow cytometry using a FACSCantoII. Fluorescence data were analyzed using FlowJo software.

RESULTS

Selected DARPins bind to EGFR on A431 cells – Since the DARPins were selected against recombinant purified EGFR ectodomain, we first assessed their binding to the native target expressed on A431 cells. This cell line shows a high overexpression of EGFR (~$3 \cdot 10^6$ receptors/cell) (46). A431 cells were incubated with DARPin_sfGFP fusion proteins, and the subsequent change in fluorescence signal was measured using flow cytometry. It was shown that all DARPins and cetuximab elicited a shift in the fluorescence signal significantly greater than that of the negative control DARPin Off7_sfGFP and of sfGFP alone (Suppl. Fig. S1).

DARPin_sfGFP fusion proteins were competed with EGF, cetuximab and unfused DARPins without GFP to verify specific binding and determine possible overlapping binding epitopes. DARPins E01, E67 and E68 could be competed with EGF as well as with cetuximab and with one another, whereas DARPin E69 could only be competed with E69 itself (Fig. 1A). Thus, the binding epitope of E01, E67 and E68 must at least partly overlap with that of

cetuximab and EGF, while E69 binds to an epitope located elsewhere.

A431 cell proliferation is inhibited by monovalent DARPins – The influence of DARPins on A431 cell viability was tested by using XTT assays as well as clonogenic assays. Cetuximab decreased cell growth by 30% in XTT assays at 100 nM. DARPins E01, E67 and E68 decreased cell viability to almost the same level as cetuximab, albeit at higher DARPin concentrations. In contrast, E69 did not show any influence on cell viability, nor did the negative control DARPin Off7 (Fig. 1B).

In the clonogenic assays, DARPins E01, E67 and E68 slightly inhibited the formation of colonies compared to cetuximab, whereas E69 and Off7 did not affect colony formation (Fig. 1C). Thus, the growth-inhibitory effect on A431 viability was restricted to DARPins E01, E67 and E68, which all share an overlapping epitope with cetuximab.

After 24 h incubation, the effect of DARPins on the cell cycle was assessed by staining the cells' DNA with propidium iodide followed by flow cytometric analysis. DARPins E01, E68, and, to a lesser extent, E67 were found to induce G1-arrest, comparable to the effect of cetuximab (Fig. 1D). The effect of these DARPins on the cell cycle was specific, as both the negative control DARPin Off7 and DARPin E69 did not appear to have an effect.

Epitope mapping of DARPins – From the competition experiments in flow cytometry (Table I), it could be inferred that DARPins E01, E67, and E68 bind to domain III of EGFR: they competed with both cetuximab and EGF for binding (9). However, the competition data did not lead to any information on the E69 epitope, since it could not be competed with any of the other DARPins or with cetuximab. Therefore, domain-level epitope mapping was first performed on E69 by using EGFR fragments displayed on the surface of yeast (39). Previously, it had been found that the full wild-type ectodomain of EGFR is not correctly displayed on the surface of yeast, but the mutant 404SG is (42). 404SG contains two point mutations in domain I (A62T and L69H) as well as two point mutations in domain III (F380S and S418G). The 404SG EGFR ectodomain mutant was used for both domain-level and subsequent fine epitope mapping. E01, E67, and E68 bound to yeast-displayed 404SG, with E67 giving a lower binding signal, possibly due to the mutations in 404SG (data not shown).

E69 showed binding to 404SG and EGFR 1-294, and very slight binding to EGFR 1-176 (Suppl. Table SI). However, no binding to EGFR 1-124 was detected. Therefore, it appeared that E69 bound to either domain I or domain II. However, since it cannot be excluded that fragments not showing E69 binding could be misfolded, from these experiments the location of the epitope can therefore only be specified to lie between residues 1 and 294. Additional competition experiments were performed with mAbs 199.12 and ICR10, which bind to domain I (39). DARPin E69 competed with these antibodies for binding to 404SG on the surface of yeast (data not shown), suggesting a domain I epitope for E69. Indeed, the fine mapping of the epitope confirmed this assignment (see below).

DARPins E01, E68 and E69 were selected for further fine epitope mapping, since they bind to different epitopes. The results are summarized in Fig. 2, showing the binding epitopes mapped onto the EGF-bound active conformation of the receptor. For defining the epitopes at residue level resolution, a library of single point mutants of 404SG was created; this library was sorted for loss of binding to the DARPin being mapped in order to determine the residues important for DARPin binding.

Besides sorting for a loss of binding, the library must also be sorted for retention of conformation, i.e. to ensure that all mutants being assessed are correctly folded. For this purpose, the EGFR library was sorted for positive binding to the conformation-specific mAb 528 (an anti-domain III antibody) and, subsequently, for loss of binding to E01 and E68. From each enriched population 48 clones were sequenced, yielding 14 residues for both epitopes. As shown in Suppl. Table SII many residues were shared between E01 and E68. Mutants Q408H, H409Y, Q411K, K465I, and G471D showed a loss of E01 binding and were tested against E68. These variants retained their E68 binding. Conversely, mutant Q348H showed a loss of E68 binding, but retained its E01 binding. Other mutants, analyzed for their loss of binding to one DARPin (F412V, A415E, I438K, K463E/I/N/T, K465E, I467M/T, N469D) were not assayed for loss of binding to the other DARPin. G418 was identified as an epitope residue for both E01 and E68, but the interpretation of these data may be ambiguous since this residue was originally mutated from serine to glycine in the 404SG variant. The epitopes of E01 and E68 are shown in Fig. 2A.

As expected, both DARPins bind to domain III. Many epitope residues are shared with cetuximab, which is consistent with the competition data (Table I). In addition, a DARPin bound to epitopes of E01 and E68 would appear to sterically clash with the EGF ligand, suggesting a mechanism for the ability of these DARPins to inhibit the growth of A431 cells.

For the mapping of E69, the EGFR mutant library was first sorted for binding to mAb EGFR1 to remove misfolded EGFR mutants. Then, after three sorts for loss of binding to E69, enriched populations were sequenced; from 98 clones, the epitope of E69 could be localized to 10 residues in domain I (Table III). The E69 epitope is shown in Fig. 2B. Fig. 2C illustrates the relative orientation of E01 and E69.

Bispecific DARPins affect A431 cell viability and proliferation similar to cetuximab – As several studies previously reported cooperative effects of mAb combinations (31, 32, 47, 48), we constructed bispecific multivalent molecules to further optimize the therapeutic potential of the DARPins by increasing the avidity. Since the epitopes of the four DARPins were mapped, two DARPins targeting different epitopes were chosen. E01, having the highest affinity, and E69 were combined in a bivalent construct with a flexible $(Gly_4Ser)_2$ linker (termed E01_GS_E69 and E69_GS_E01, Fig. 3A). A more rigid construct that was at the same time bispecific and bivalent for each epitope was created by making use of a leucine zipper (termed E69_LZx_E01 and E01_LZx_E69, Fig. 3B). For this format, different linker lengths were tested between the DARPins and the leucine zipper (Fig. 5A); the shortest linker, consisting of G_3S (variant LZ3), proved to be the best (Fig. 5).

The bispecific constructs without leucine zipper were able to affect cell viability and induce G1 arrest to the same extent as the 1:1 molecular mixture of the monovalent DARPins E01 and E69, and cetuximab (Fig. 4A and C). This suggests that the observed effect is mainly due to E01 binding, as E69 itself has no effect. The slightly better performance of E01_GS_E69 and E69_GS_E01 than the E01/E69 mixture at intermediate concentrations is probably a simple avidity effect. In contrast, in the clonogenic assay, E01_GS_E69 and E69_GS_E01 were not able to inhibit colony formation to a significant extent (Fig. 4B). Considering the experimental error, no significant difference in the inhibition of A431 proliferation was seen between the two orientations in any of the assays.

In contrast, for the leucine zipper constructs, a difference in the biological activity was clearly observed between both orientations (Fig. 5B, C and D). The E69_LZ3_E01 molecule was capable of inhibiting cell viability already at low concentrations, whereas the opposite orientation E01_LZ3_E69 was not. Differences in the extent of cell cycle arrest were seen as well (Fig. 5F and G). It was shown by FACS competition measurements that E69_LZ3_E01 blocks epitopes of labeled E69 or labeled E01 efficiently, while E01_LZ3_E69 does not (Suppl. Fig. S2). Since the cells were exposed to the multivalent DARPins at 4°C for 30 min, it is unlikely that significant internalization was triggered. The DARPins were incubated in a 1:1 molar ratio with EGFR expressed on A431 cells, and it might well be that not all epitopes were covered in this experiment. Nonetheless, it is clear that E69_LZ3_E01 more efficiently blocks binding of either labeled monovalent DARPin, suggesting that its binding sites are arranged for a better fit to the EGFR structure than E01_LZ3_E69.

In addition, E69_LZ3_E01 was more effective in inhibiting A431 proliferation in the clonogenic assay than cetuximab with an IC_{50} of approximately 100 nM (Fig. 5D and E). It is interesting to note that the decrease in proliferation is very gradual with concentration. This is consistent with the idea that only a small number of receptors need to be phosphorylated in order to initiate significant downstream signaling (49). To further investigate these effects, A431 cells were treated with the DARPins and the effect on cell signaling was examined by Western blot. In addition to E01, all bispecific DARPins were able to inhibit phosphorylation of EGFR (Y1068) (Fig. 6A). All bispecific DARPins were more effective in the inhibition of the phosphorylation of ERK (p44/p42) than cetuximab (Fig. 6B). In the case of Akt, both cetuximab and E69_LZ3_E01 were effective in inhibiting phosphorylation (Fig. 6C); in contrast, the other DARPins were not as effective.

Interestingly, when examining total EGFR levels, it was found that E69_LZ3_E01 dramatically reduced total EGFR (Fig. 6A); the other constructs and cetuximab did not show this effect.

E69_LZ3_E01 effectively inhibits receptor recycling – Since the amount of total EGFR was

reduced in Western blot after treating A431 cells with E69_LZ3_E01, EGFR receptor recycling was investigated according to (32). E69_LZ3_E01 and monovalent E01 were coupled to Alexa Fluor 488 C_5-maleimide. The fluorescence originating from internalized DARPins was measured after quenching the fluorescence signal from DARPins that were not internalized with an anti-Alexa antibody. In addition, fluorescence from DARPins that would recycle back to the cell surface together with EGFR was competed with an excess of unlabeled DARPin. Monovalent E01 both alone and in combination with monovalent E69 was not able to inhibit receptor recycling. In contrast, E69_LZ3_E01 effectively inhibited receptor recycling (Fig. 7A and C).

This finding was supported by a second assay, in which monensin was used as a positive control to inhibit protein transport and EGFR recycling (50). The surface EGFR level was assessed after treatment with E69_LZ3_E01 and the positive control monensin. As expected, the surface EGFR level was decreased after treatment with either monensin or E69_LZ3_E01 (Fig. 7B). Thus, E69_LZ3_E01 clearly inhibits receptor recycling, which corroborates with the down-regulation of EGFR seen in Western blot.

DISCUSSION

The EGF receptor is a valuable target for tumor therapy (15). While the clinical benefits of monoclonal anti-EGFR antibodies in the IgG format have so far been rather modest, it is likely that different targeting molecules with novel effector functions can ultimately lead to improved tumor therapies. Ideally, any such targeting molecule should be able, in addition to the effect of any potential payload, to inhibit signaling via EGFR. Since DARPins are particularly robust and thus suitable for such tumor targeting constructs (27), we investigated the inhibitory properties of previously selected anti-EGFR DARPins (21) on the well-characterized A431 cell line (30). The results were correlated with a determination of their conformational epitopes at amino acid-level resolution. We then combined two non-competitive DARPins in different bispecific formats to further optimize the biological activity.

DARPins with (sub)nanomolar affinities had been selected against the purified extracellular region of EGFR (sEGFR) (21) (Table I). To address the question whether the selected DARPins would have biological effects similar to cetuximab, we carried out a number of cell-based assays. The anti-EGFR DARPins fall into two groups. DARPins E01, E67 and E68 decrease cell viability and inhibit cell growth, as seen in XTT and clonogenic assays, and induce G1-arrest; DARPin E69 has no such effect (Fig. 1). In addition, the negative control DARPin Off7 shows no biological activity, indicating that the observed effects of DARPins E01, E67 and E68 on A431 cells are EGFR-specific.

Our flow cytometry competition experiments showed that DARPins E01, E67 and E68 competed with cetuximab as well as EGF for binding, whereas E69 did not (Table I). These findings are consistent with the results from epitope mapping by yeast surface display of EGFR (39, 40) (Fig. 2). An error-prone library of sEGFR ectodomain variants was displayed on the surface of yeast and was selected for loss of binding to the DARPins. This method has the advantage that non-linear epitopes can be precisely mapped at residue resolution. Since the library was first sorted for binding to conformation-specific control antibodies binding to the same domain, loss of binding is not simply due to a loss of structure in the identified EGFR mutants.

Using this method, we determined that the epitopes of DARPins E01 and E68 are located exclusively on domain III (Suppl. Table SIII). Similar to cetuximab, E01 and E68 bind epitopes located near the C-terminal end of domain III. Binding of DARPins E01 and E68 interferes with hydrophobic interactions of the receptor with the ligand. Both DARPins bind to residue A415, which is located in a hydrophobic pocket; compared to cetuximab, which does not bind to this residue, the DARPins are packed more deeply into the binding pocket in this region of EGFR. In addition, the hydrogen bond of Q384 of EGFR with the main chain carbonyl and amide groups of Q43 and R45 of EGF and the stabilization of the C-terminal carboxyl group of EGF by K465 of EGFR are disrupted by DARPin binding. Thus, E01 and E68 exhibit their activity via physically blocking the receptor-ligand interaction.

The E69 epitope was localized to ten residues in EGFR domain I (Suppl. Tables SI and SII). EGF does interact with domain I, although these residues are located towards the N-terminal end of domain I (4); the epitope for E69 is in fact located near the C-terminal

end of domain I. Based on the epitope residues determined by the yeast display method, it does not appear that EGF binding would be physically blocked by this DARPin. Consistent with our data on the E69 epitope, we determined that cell proliferation and survival are not affected by treatment with DARPin E69.

Cetuximab has a mechanism of action similar to E01 and E68. This mAb was co-crystallized with the receptor; the 3D structure revealed that cetuximab exerts its growth inhibitory activity by partly occluding an epitope overlapping with the EGF-binding site on domain III of EGFR, while the V_H region of the antibody sterically blocks domain I (9). In this way, the receptor is prevented from adopting the open conformation required for receptor dimerization and activation. In the past, a number of other anti-EGFR mAbs has been developed by immunizing mice with human EGFR-overexpressing tumor cells (51–54). The antibody IMC-11F8, which has been selected from a Fab library by competing against cetuximab and screening for inhibition of EGFR signaling inhibition, was found to bind to the same epitope as cetuximab in the same orientation (55). Matuzumab, the humanized form of the murine antibody mAb425, binds to a different epitope on domain III of EGFR and does not block EGF binding, but prevents the conformational change of the receptor required for dimerization (56). mAb806 and mAb175, which have been raised against a deletion variant of EGFR, recognize an epitope in domain II, which is buried in the wild-type receptor in the tethered, non-activated conformation (57). Apparently, this epitope is recognized on wild-type receptors on tumor cells, but not on normal cells. Other antibodies against EGFR are in development, whose epitopes have not yet been crystallographically defined (58).

The activity of DARPins E01, E67, and E68 at high concentrations is comparable to that of cetuximab. However, despite their high affinity for the target (21) higher concentrations are needed to affect the short-term cell viability in XTT assays. Cetuximab has an avidity of 1 nM on A431 cells (47)), but its bivalent nature has been shown to induce receptor internalization (47, 59), and antibody-induced EGFR dimerization was necessary for down-regulation of EGFR. This antibody-induced dimerization does not lead to receptor activation. The monovalent Fab' derived from cetuximab (47, 60) had a less pronounced effect on cell proliferation and did not induce receptor down-regulation (47). However, the monovalent Fab' was still able to inhibit receptor phosphorylation, indicating that inhibition of the signaling pathways is not dependent on receptor down-regulation which would require bivalency (61). E01 similarly inhibits receptor phosphorylation (Fig. 5), but hardly affects ERK/Akt downstream signaling. It has been shown previously that signaling through EGFR can still occur despite the absence of EGFR phosphorylation (62–64). ERK and Akt can still be phosphorylated, though other receptors and pathways might be involved. In addition, only a small number of receptors need to be phosphorylated in order to initiate significant downstream signaling (49). Possibly, bivalent binding to the receptor is a prerequisite to abolish this effect.

Thus, to optimize the effect of the DARPins, we constructed bivalent and tetravalent binders. It was recently shown that certain combinations of mAbs are superior in controlling tumor growth by synergistically inhibiting receptor recycling after internalization (31, 32, 65, 66). In particular, mAbs engaging distinct epitopes accelerated net internalization by cross-linking EGFR on the cellular surface. As the previously selected group of DARPins targeted two distinct epitopes, two of these DARPins were combined: E01, having the highest affinity, and E69, targeting an epitope located on domain I, were chosen. Bispecific DARPins were constructed with a flexible linker, as well as with a leucine zipper. Bispecific DARPins connected through a flexible linker more effectively inhibited A431 proliferation than the monovalent constructs, as seen in XTT assays, and induced G1 arrest (Fig. 4). Both orientations showed inhibition of phosphorylation of EGFR and ERK1/2 (Fig. 6). However, the Akt pathway was only affected to a lesser extent in comparison to the MAPK pathway. Since the A431 cell line depends both on the MAPK and Akt pathways for cell survival and proliferation (43), inhibition of long-term cell viability was limited, as confirmed by the clonogenic assay.

Interestingly, the E69_LZ3_E01 variant was particularly effective in inhibiting A431 proliferation. In this molecule, each DARPin is also bivalent (Fig. 3B). The clonogenic assay showed a significant decrease in the survival fraction. Western blot analysis revealed that phosphorylation of EGFR and the signaling molecules ERK1/2 and Akt was inhibited, thus

affecting A431 cell viability and survival. The reverse orientation, E01_LZ3_E69, showed hardly any biological activity on A431 cells. Though E01_LZ3_E69 was able to bind to EGFR expressed on A431 cells, this orientation did not block epitopes on EGFR as efficiently as E69_LZ3_E01 (Suppl. Fig. S2). Thus, A431 cell proliferation and survival were not particularly affected by E01_LZ3_E69. A similar observation was made by Roovers *et al*., who combined two nanobodies both with epitopes located on domain III (67). They found that bispecific nanobody 9G8-7D12 induced EGFR phosphorylation and A431 cell proliferation; in contrast, the reverse orientation 7D12-9G8 did not cause receptor activation and therefore functioned as an antagonist.

In addition to the direct inhibition of signaling, total EGFR was significantly decreased after E69_LZ3_E01 treatment. To understand the mechanism of this effect, internalization and recycling assays according to (32) were performed. It was found that E69_LZ3_E01 efficiently prevented recycling of EGFR to the cellular surface, which was compared with the effect of the receptor recycling inhibitor monensin (Fig. 7). Monovalent E01 and E69 were unable to inhibit receptor recycling.

In this work, we have combined an EGFR domain I-binder with a domain III-binder where each of the binders is also bivalent. Spangler *et al.* showed that a combination of two domain III-binders was the most effective in receptor down-regulation, but found that a triepitopic format was the most optimal for biological activity (32, 68). However, the extent of receptor down-regulation induced by binding molecules likely depends on the receptor conformation and orientation. On A431 cells, EGFR is present in at least three different states, which differ in their degree of nanoscale and submicron scale clustering (69). In particular, the presence of higher order EGFR clusters in this cell line is distinctly different from the situation in which EGFR is expressed at a normal level; in the absence of high overexpression, EGFR is clustered in lower order clusters, i.e. monomers and dimers (69). Since E69_LZ3_E01 treatment down-regulates EGFR to a great extent, these DARPins, homodimerized via the leucine zipper, must be able to reach more than one EGFR molecule. In theory, the bispecific binders without leucine zipper might also be able to induce receptor clustering, but the short linker used in this study is most likely not suited since no change in surface EGFR was seen (Fig. 6). Thus, these molecules seem to contact only one EGFR molecule at a time. In summary, the leucine zipper seems to be the optimal construct; in this format, both DARPins are combined in one construct and are each bivalent, which makes expression convenient and straightforward.

In conclusion, we have established that three of the DARPins presented in this work exhibit a growth-inhibitory effect on A431 cells *in vitro*. By mapping their epitopes, we can infer that the biologically active DARPins E01 and E68 compete with the ligand binding site on EGFR without themselves causing a signal, thus blocking the receptor — a very useful feature of any EGFR targeting protein, even when carrying other effector functions. By linking DARPins E01 and E69, both targeting distinct epitopes, in a bispecific and bivalent format, the biological activity was significantly improved. The E69_LZ3_E01 construct could, in addition to its competitive inhibition of signaling, cross-link receptors on the cellular surface, leading to EGFR down-regulation. DARPin E69_LZ3_E01 can therefore form the starting point for the addition of novel functions by linking other effector domains. In stark contrast to antibodies, such constructs can be prepared with very high yields in bacteria. Such DARPins may thus be able to form building blocks for future therapeutics.

REFERENCES

1. Mendelsohn, J. and Baselga, J. (2003) *J. Clin. Oncol.* **21**, 2787-2799.
2. Fuller, S. J., Sivarajah, K., and Sugden, P. H. (2008) *J. Mol. Cell. Cardiol.* **44**, 831-854.
3. Scaltriti, M. and Baselga, J. (2006) *Clin. Cancer Res.* **12**, 5268-5272
4. Ogiso, H., Ishitani, R., Nureki, O., Fukai, S., Yamanaka, M., Kim, J.-H., Saito, K., Sakamoto, A., Inoue, M., Shirouzu, M., and Yokoyama, S. (2002) *Cell* **110**, 775-787.
5. Higashiyama, S., Iwabuki, H., Morimoto, C., Hieda, M., Inoue, H., and Matsushita, N. (2008) *Cancer Sci.* **99**, 214-220.

6. Sergina, N. V. and Moasser, M. M. (2007) *Trends Mol. Med.* **13**, 527-534.
7. Burgess, A. W. (2008) *Growth Factors* **26**, 263-274
8. Zhang, X., Gureasko, J., Shen, K., Cole, P. A., and Kuriyan, J. (2006) *Cell* **125**, 1137-1149.
9. Li, S., Schmitz, K. R., Jeffrey, P. D., Wiltzius, J. J. W., Kussie, P., and Ferguson, K. M. (2005) *Cancer Cell* **7**, 301-311.
10. Holbro, T. and Hynes, N. E. (2004) *Annu. Rev. Pharmacol. Toxicol.* **44**, 195-217.
11. Wiley, H. S. (2003) *Exp. Cell Res.* **284**, 78-88.
12. Hildebrandt, B., le Coutre, P., Nicolaou, A., Köble, K., Riess, H., and Dörken, B. (2007) *Recent Res. Cancer Res.* **176**, 135-143.
13. Mendelsohn, J. (2002) *J. Clin. Oncol.* **20**, 1s-13s.
14. Hynes, N. E. and MacDonald, G. (2009) *Curr. Opin. Cell Biol.* **21**, 177-184.
15. Dassonville, O., Bozec, A., Fischel, J. L., and Milano, G. (2007) *Crit. Rev. Oncol. Hematol.* **62**, 53-61.
16. Friedländer, E., Barok, M., Szöllosi, J., and Vereb, G. (2008) *Immunol. Lett.* **116**, 126-140.
17. Patel, D., Bassi, R., Hooper, A., Prewett, M., Hicklin, D. J., and Kang, X. (2009) *Int. J. Oncol.* **34**, 25-32.
18. Boersma, Y. L. and Plückthun, A. (2011) *Curr. Opin. Biotechnol.*, doi:10.1016/j.copbio.2011.06.004.
19. Löfblom, J., Frejd, F. Y., and Ståhl, S. (2011) *Curr. Opin. Biotechnol.*, doi:10.1016/j.copbio.2011.06.002.
20. Binz, H. K., Amstutz, P., Kohl, A., Stumpp, M. T., Briand, C., Forrer, P., Grutter, M. G., and Plückthun, A. (2004) *Nat. Biotechnol.* **22**, 575-582
21. Steiner, D., Forrer, P., and Plückthun, A. (2008) *J. Mol. Biol* **382**, 1211-1227.
22. Zahnd, C., Wyler, E., Schwenk, J. M., Steiner, D., Lawrence, M. C., McKern, N. M., Pecorari, F., Ward, C. W., Joos, T. O., and Plückthun, A. (2007) *J. Mol. Biol.* **369**, 1015-1028
23. Huber, T., Steiner, D., Rothlisberger, D., and Plückthun, A. (2007) *J. Struct. Biol.* **159**, 206-221
24. Kawe, M., Forrer, P., Amstutz, P., and Plückthun, A. (2006) *J. Biol. Chem.* **281**, 40252-40263
25. Zahnd, C., Pecorari, F., Straumann, N., Wyler, E., and Plückthun, A. (2006) *J. Biol. Chem.* **281**, 35167-35175
26. Zahnd, C., Amstutz, P., and Plückthun, A. (2007) *Nat. Methods* **4**, 269-279.
27. Zahnd, C., Kawe, M., Stumpp, M. T., de Pasquale, C., Tamaskovic, R., Nagy-Davidescu, G., Dreier, B., Schibli, R., Binz, H. K., Waibel, R., and Plückthun, A. (2010) *Cancer Res.* **70**, 1595-605.
28. Winkler, J., Martin-Killias, P., Plückthun, A., and Zangemeister-Wittke, U. (2009) *Mol. Cancer Ther.* **8**, 2674-2683.
29. Martin-Killias, P., Stefan, N., Rothschild, S., Plückthun, A., and Zangemeister-Wittke, U. (2011) *Clin. Cancer Res.* **17**, 100-110.
30. Giard, D. J., Aaronson, S. A., Todaro, G. J., Arnstein, P., Kersey, J. H., Dosik, H., and Parks, W. P. (1973) *J. Natl. Cancer Inst.* **51**, 1417-1423.
31. Friedman, L. M., Rinon, A., Schechter, B., Lyass, L., Lavi, S., Bacus, S. S., Sela, M., and Yarden, Y. (2005) *Proc. Natl. Acad. Sci. U.S.A.* **102**, 1915 -1920.
32. Spangler, J. B., Neil, J. R., Abramovitch, S., Yarden, Y., White, F. M., Lauffenburger, D. A., and Wittrup, K. D. (2010) *Proc. Natl. Acad. Sci. U.S.A.* **107**, 13252 -13257.
33. Pedelacq, J.-D., Cabantous, S., Tran, T., Terwilliger, T. C., and Waldo, G. S. (2006) *Nat. Biotechnol.* **24**, 79-88.
34. Binz, H. K., Stumpp, M. T., Forrer, P., Amstutz, P., and Pluckthun, A. (2003) *J. Mol. Biol.* **332**, 489-503
35. Janmaat, M. L., Kruyt, F. A. E., Rodriguez, J. A., and Giaccone, G. (2003) *Clin. Cancer Res.* **9**, 2316-2326.
36. Franken, N. A. P., Rodermond, H. M., Stap, J., Haveman, J., and van Bree, C. (2006) *Nat. Protoc.* **1**, 2315-2319.
37. Huang, S. M. and Harari, P. M. (2000) *Clin. Cancer Res.* **6**, 2166-2174
38. Riccardi, C. and Nicoletti, I. (2006) *Nat. Protoc.* **1**, 1458-1461.
39. Cochran, J. R., Kim, Y.-S., Olsen, M. J., Bhandari, R., and Wittrup, K. D. (2004) *J. Immunol. Methods* **287**, 147-158.

40. Chao, G., Cochran, J. R., and Wittrup, K. D. (2004) *J. Mol. Biol.* **342**, 539-550.
41. Oliphant, T., Engle, M., Nybakken, G. E., Doane, C., Johnson, S., Huang, L., Gorlatov, S., Mehlhop, E., Marri, A., Chung, K. M., Ebel, G. D., Kramer, L. D., Fremont, D. H., and Diamond, M. S. (2005) *Nat. Med.* **11**, 522-530.
42. Kim, Y.-S., Bhandari, R., Cochran, J. R., Kuriyan, J., and Wittrup, K. D. (2006) *Proteins* **62**, 1026-1035.
43. Meira, D. D., Nóbrega, I., de Almeida, V. H., Mororó, J. S., Cardoso, A. M., Silva, R. L. A., Albano, R. M., and Ferreira, C. G. (2009) *Eur. J. Cancer* **45**, 1265-1273.
44. Diaz Miqueli, A., Blanco, R., Garcia, B., Badia, T., Batista, A. E., Alonso, R., and Montero, E. (2007) *Hybridoma* **26**, 423-431.
45. Raben, D., Helfrich, B., Chan, D. C., Ciardiello, F., Zhao, L., Franklin, W., Baron, A. E., Zeng, C., Johnson, T. K., and Bunn, P. A. (2005) *Clin. Cancer Res.* **11**, 795-805
46. Kawamoto, T., Sato, J. D., Le, A., Polikoff, J., Sato, G. H., and Mendelsohn, J. (1983) *Proc. Natl. Acad. Sci. U.S.A* **80**, 1337-1341.
47. Fan, Z., Lu, Y., Wu, X., and Mendelsohn, J. (1994) *J. Biol. Chem.* **269**, 27595-27602.
48. Xu, F., Lupu, R., Rodriguez, G. C., Whitaker, R. S., Boente, M. P., Berchuck, A., Yu, Y., DeSombre, K. A., Boyer, C. M., and Bast, R. C. (1993) *Int. J. Cancer* **53**, 401-408.
49. Chen, W. W., Schoeberl, B., Jasper, P. J., Niepel, M., Nielsen, U. B., Lauffenburger, D. A., and Sorger, P. K. (2009) *Mol. Syst. Biol.* **5**, 239.
50. Felder, S., Miller, K., Moehren, G., Ullrich, A., Schlessinger, J., and Hopkins, C. R. (1990) *Cell* **61**, 623-634.
51. Parker, P. J., Young, S., Gullick, W. J., Mayes, E. L., Bennett, P., and Waterfield, M. D. (1984) *J. Biol. Chem.* **259**, 9906-9912.
52. Gill, G. N., Kawamoto, T., Cochet, C., Le, A., Sato, J. D., Masui, H., McLeod, C., and Mendelsohn, J. (1984) *J. Biol. Chem.* **259**, 7755-7760.
53. Sato, J. D., Kawamoto, T., Le, A. D., Mendelsohn, J., Polikoff, J., and Sato, G. H. (1983) *Mol. Biol. Med.* **1**, 511-529.
54. Hong, K.-W., Kim, C.-G., Lee, S.-H., Chang, K.-H., Shin, Y. W., Ryoo, K.-H., Kim, S.-H., and Kim, Y.-S. (2010) *J. Biotechnol.* **145**, 84-91.
55. Li, S., Kussie, P., and Ferguson, K. M. (2008) *Structure* **16**, 216-227.
56. Schmiedel, J., Blaukat, A., Li, S., Knöchel, T., and Ferguson, K. M. (2008) *Cancer Cell* **13**, 365-373.
57. Garrett, T. P. J., Burgess, A. W., Gan, H. K., Luwor, R. B., Cartwright, G., Walker, F., Orchard, S. G., Clayton, A. H. A., Nice, E. C., Rothacker, J., Catimel, B., Cavenee, W. K., Old, L. J., Stockert, E., Ritter, G., Adams, T. E., Hoyne, P. A., Wittrup, D., Chao, G., Cochran, J. R., Luo, C., Lou, M., Huyton, T., Xu, Y., Fairlie, W. D., Yao, S., Scott, A. M., and Johns, T. G. (2009) *Proc. Natl. Acad. Sci. U.S.A.* **106**, 5082-5087.
58. Schmitz, K. R. and Ferguson, K. M. (2009) *Exp. Cell Res.* **315**, 659-670.
59. Jaramillo, M. L., Leon, Z., Grothe, S., Paul-Roc, B., Abulrob, A., and O'Connor McCourt, M. (2006) *Exp. Cell Res.* **312**, 2778-2790.
60. Fan, Z., Masui, H., Altas, I., and Mendelsohn, J. (1993) *Cancer Res.* **53**, 4322-4328.
61. Fan, Z., Mendelsohn, J., Masui, H., and Kumar, R. (1993) *J. Biol. Chem.* **268**, 21073-21079.
62. Decker, S. J. (1993) *J. Biol. Chem* **268**, 9176-9179.
63. Gotoh, N., Tojo, A., Muroya, K., Hashimoto, Y., Hattori, S., Nakamura, S., Takenawa, T., Yazaki, Y., and Shibuya, M. (1994) *Proc. Natl. Acad. Sci. U.S.A* **91**, 167-171
64. Maegawa, M., Arao, T., Yokote, H., Matsumoto, K., Kudo, K., Tanaka, K., Kaneda, H., Fujita, Y., Ito, F., and Nishio, K. (2009) *Cancer Sci.* **100**, 552-557.
65. Pedersen, M. W., Jacobsen, H. J., Koefoed, K., Hey, A., Pyke, C., Haurum, J. S., and Kragh, M. (2010) *Cancer Res.* **70**, 588 -597.
66. Kamat, V., Donaldson, J. M., Kari, C., Quadros, M. R. D., Lelkes, P. I., Chaiken, I., Cocklin, S., Williams, J. C., Papazoglou, E., and Rodeck, U. (2008) *Cancer Biol. Ther.* **7**, 726-733.
67. Roovers, R. C., Vosjan, M. J. W. ., Laeremans, T., el Khoulati, R., de Bruin, R. C. G., Ferguson, K. M., Verkleij, A. J., van Dongen, G. A. M. ., and van Bergen en Henegouwen, P. M. P. *Int. J. Cancer*, doi/10.1002/ijc.26145.
68. Spangler, J. B., Manzari, M. T., Rosalia, E. K., Chen, T. F., and Wittrup, K. D. (2011) *Submitted*

69. Clayton, A. H. A., Tavarnesi, M. L., and Johns, T. G. (2007) *Biochemistry* **46**, 4589-4597.

FOOTNOTES

The authors would like to thank Dr. A. Honegger for her help with Fig. 3. This work was funded by the Dutch Organization for Scientific Research (NWO) (Rubicon postdoctoral grant 680-50-0704) to Y.L.B., Oncosuisse (OCS-02128-08-2007) to A.P., and NIH grant CA96504 to G.C. and K.D.W.

Abbreviations used are: EGFR, epidermal growth factor receptor; DARPin, designed ankyrin repeat protein; XTT, 2,3-bis-(2-methoxy-4-nitro-5-sulfophenyl)-2H-tetrazolium-5-carboxanilide; mAb, monoclonal antibody; LZ, leucine zipper; GS, $(G_4S)_2$-linker.

FIGURE LEGENDS

FIGURE 1. Epitope comparison and biological effects of monovalent DARPins binding to A431 cells. Cetuximab is abbreviated as Cet. Each symbol or bar represents the average of three data points. (*A*) Epitope comparison using flow cytometry. DARPins on the x-axis were genetically fused to sfGFP. A431 cells were incubated with 100 nM sfGFP-tagged DARPin and 1 µM unlabeled DARPin, cetuximab or EGF (denoted by the differently shaded bars). E69 is the only DARPin that cannot be competed with any other DARPin, only with itself. (*B*) Inhibition of cell viability as determined by XTT assays. Cells were treated for 72 h with different concentrations of DARPins. DARPins E01, E67 and E68 affect the cell proliferation (Student's t-test $p<0.05$ compared to untreated cells), whereas E69 and negative control Off7 do not. (*C*) Inhibition of cell proliferation as determined by clonogenic assays. A431 cells were treated for 7 days with 100 nM DARPin or 100 nM cetuximab, after which the medium was changed and cells were allowed to grow for another 7 days. E01, E67 and E68 slightly inhibited cell proliferation, while E69 did not. (*D*) Cell cycle distribution. A431 cells were treated for 24 h with 100 nM DARPin or 100 nM cetuximab, after which cells were stained with propidium iodide and measured by flow cytometry. E01, E67 and E68 induced G1-arrest (Student's t-test $p<0.05$ compared to untreated cells), whereas E69 did not affect A431 cells.

FIGURE 2. Epitopes of DARPins on EGFR and their spatial relation relative to bound EGF. (*A*) Comparison of the epitopes of E01, E68 and cetuximab on domain III of EGFR. EGFR residues involved in DARPin/cetuximab binding are in red, EGF in green stick representation. (*B*) Epitope of E69. EGFR residues involved in E69 binding are depicted in red, EGF is in green stick representation. (*C*) Overview of epitopes of E01 and E69. EGFR is shown in ribbon representation, with domain I in red, domain II in green, and domain III in blue, and part of domain IV in grey. The EGF ligand is shown in yellow in stick representation. Residues involved in E69 binding are shown in CPK representation in pink (domain I), and residues involved in either E01 or E68 binding are shown in CPK representation in cyan (domain III).

FIGURE 3. Representations of the bispecific DARPins used in this work. (*A*) Model of the structure of E69_GS_E01. E69 (red) and E01 (blue) are both represented as cartoon, whereas the flexible linker (yellow) is represented in sticks. (*B*) Stick model of the structure of E69_LZ3_E01. E69 at the N-terminus is depicted in red, E01 in blue, the leucine zipper in green, and the linkers in yellow.

FIGURE 4. Biological activity of bispecific DARPins with a flexible linker. Cetuximab is abbreviated as Cet. Each symbol or bar represents the average of three data points. (*A*) Inhibition of cell viability as determined by XTT assays. Cells were treated for 72 h with different concentrations of bivalent DARPins. A 1:1 mixture of DARPins E01 and E69, E01_GS_E69 and E69_GS_E01 affect the cell proliferation similar to cetuximab (Student's t-test $p<0.05$ compared to untreated cells); negative control DARPin Off7 does not. (*B*) Inhibition of cell proliferation as determined by clonogenic assays. A431 cells were treated for 7 days with 100 nM DARPin or 100 nM cetuximab, after which the medium was changed and cells were allowed to grow for another 7 days. (*C*) Cell cycle distribution. A431 cells were treated for 24 h with 100 nM DARPin or 100 nM cetuximab, after which cells were stained with propidium iodide and measured by flow cytometry.

FIGURE 5. Biological activity of bispecific DARPins connected with a leucine zipper through different linkers. Cetuximab is abbreviated as Cet. Each symbol or bar represents the average of three data points. (*A*) Schematic overview of the constructs with different linker lengths. (*B*) Inhibition of A431 cell viability as determined by XTT assays. Cells were treated for 72 h with different concentrations of bispecific DARPins with flexible Gly-Ser linker or dimerizing leucine zipper, with E01 at the N-terminus and E69 at the C-terminus. E01_LZ1_E69 and E01_LZ2_E69 affect cell proliferation similar to cetuximab (Student's t-test $p<0.05$ compared to untreated cells), whereas the negative control Off7 and E01_LZ3_E69 do not affect cell proliferation. (*C*) Inhibition of A431 cell viability as determined by XTT assays. Cells were treated for 72 h with different concentrations of bispecific DARPins with flexible Gly-Ser linker or dimerizing leucine zipper, with E69 at the N-terminus and E01 at the C-terminus. E69_LZ1_E01 and E69_LZ3_E01 affect cell proliferation

similar to cetuximab (Student's t-test $p<0.05$ compared to untreated cells), whereas negative control Off7 does not affect cell proliferation. DARPin E69_LZ2_E01 does affect cell proliferation, but to a lesser extent. (*D*) Inhibition of cell proliferation as determined by clonogenic assays. A431 cells were treated for 7 days with 100 nM DARPin or 100 nM cetuximab, after which the medium was changed and cells were allowed to grow for another 7 days. E69_LZ3_E01 significantly inhibited cell proliferation (Student's t-test $p<0.02$ compared to untreated cells), whereas the other constructs had a less pronounced effect on cell proliferation. (*E*) Inhibition of cell proliferation as determined by clonogenic assays at different concentrations. A431 cells were treated with different concentrations of DARPin or cetuximab for 7 days, after which the medium was changed and cells were allowed to grow for another 7 days. Both cetuximab and E69_LZ3_E01 significantly inhibited cell proliferation (Student's t-test $p<0.02$ and $p<0.01$, respectively), whereas negative control Off7 did not show an effect. The IC_{50} of E69_LZ3_E01 as determined from this graph is approximately 100 nM. (*F, G*) Cell cycle distribution. A431 cells were treated for 24 h with 100 nM bispecific DARPin with dimerizing leucine zipper or with 100 nM cetuximab, after which cells were stained with propidium iodide and measured by flow cytometry. The bispecific DARPins induced G1-arrest (Student's t-test $p<0.05$ compared to untreated cells), while E69_LZ3_E01 in particular significantly induced G1-arrest (Student's t-test $p<0.02$ compared to untreated cells).

FIGURE 6. Effect of DARPin treatment on downstream signaling. A431 cells were treated for 24 h with 100 nM cetuximab or 100 nM DARPin. Cells were then stimulated with 10 ng/ml EGF, except cells from sample "*None -EGF*". Cell lysate corresponding to 20 µg protein was loaded onto an SDS-PAGE gel; proteins were then transferred by Western blot and detected by a fluorescently labeled secondary antibody. A digital image of the fluorescently stained Western blot is shown above and a quantitation of the band intensity below. (*A*) Detection of EGFR and pEGFR (Y1068). E69_LZ3_E01 dramatically reduces total EGFR. (*B*) Detection of ERK1/2 and pERK1/2 (T202/Y204). E01_GS_E69, E69_GS_E01 and E69_LZ3_E01 inhibit ERK1/2 phosphorylation dramatically. (*C*) Detection of Akt and pAkt (S473). E69_LZ3_E01 inhibits Akt phosphorylation to some extent.

FIGURE 7. EGFR down regulation by E69_LZ3_E01 is caused by an inhibition of receptor recycling. (*A*) A431 cells were treated for 2 h with 100 nM DARPin_Alexa Fluor 488 at 37°C to allow for internalization of the EGFR:DARPin complex. Residual fluorescence outside the cell was quenched by an anti-Alexa quenching antibody, while fluorescence from recycled EGFR:DARPin complexes was chased by unlabeled DARPin. The fluorescence signal from internalized receptor-DARPin complex was measured and compared to an untreated control. E69_LZ3_E01 was able to inhibit recycling back to the surface, whereas E01 alone as well as in combination with E69 did not. (*B*) A431 cells were treated for 20 min with the receptor recycling inhibitor monensin or with E69_LZ3_E01. At the indicated time points, residual surface EGFR was analyzed by flow cytometry. E69_LZ3_E01 was able to inhibit receptor recycling to the same extent as monensin. (*C*) Schematic overview of the biological effect of DARPin E69_LZ3_E01 on A431 cells overexpressing EGFR. DARPin E69 is depicted in red, whereas E01 is depicted in blue; the DARPins are connected via a leucine zipper. Upon treatment of A431 cells with the DARPin, EGFR on the cellular surface will organize in clusters. These clusters are internalized via clathrin-coated pits into the early endosome. Normally, EGFR will be recycled back to the cellular surface via the recycling endosome; in the case of E69_LZ3_E01, however, recycling is inhibited and total surface EGFR is diminished. This has a strong impact on cell proliferation and downstream signaling events.

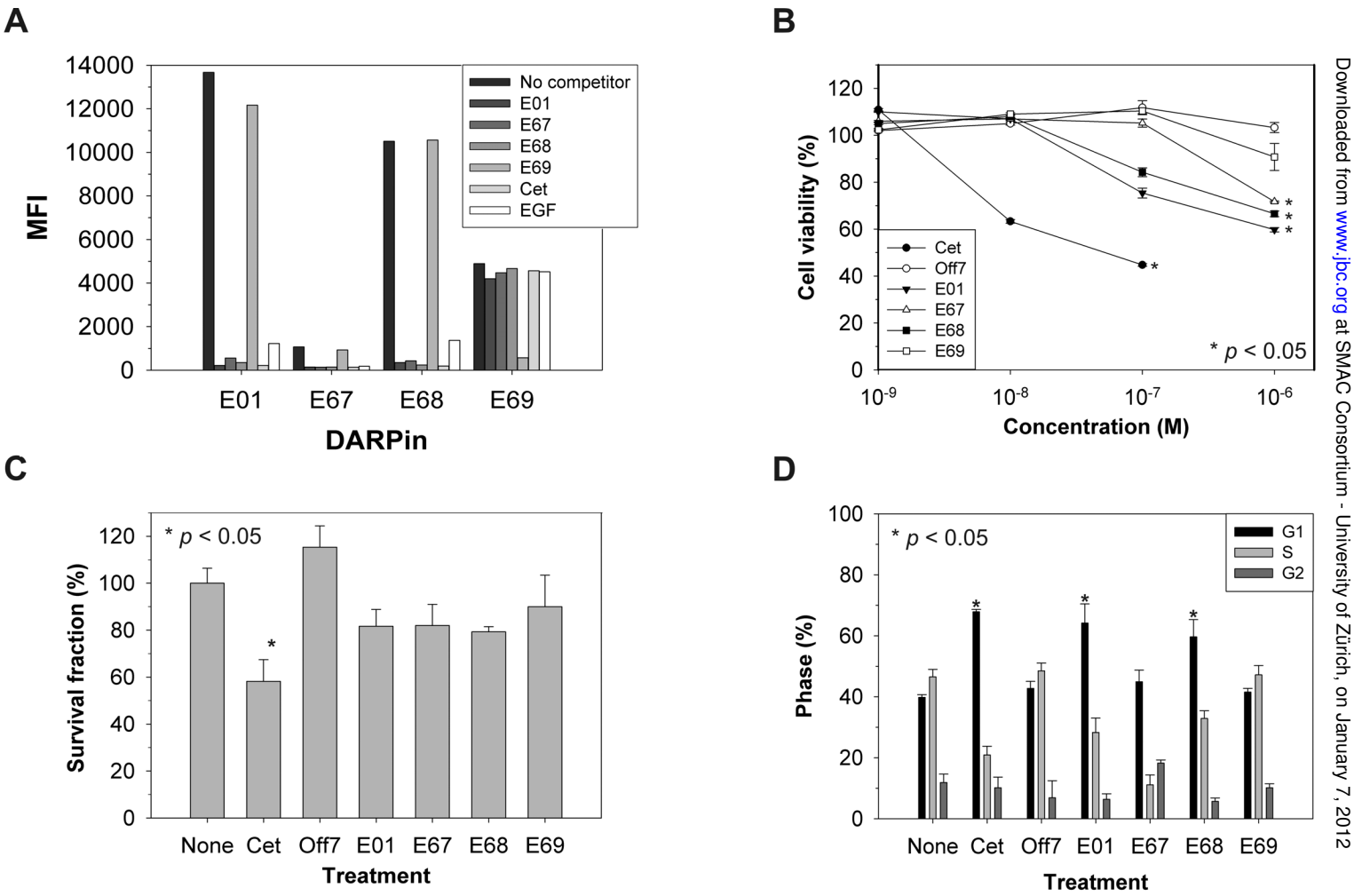

Figure 1

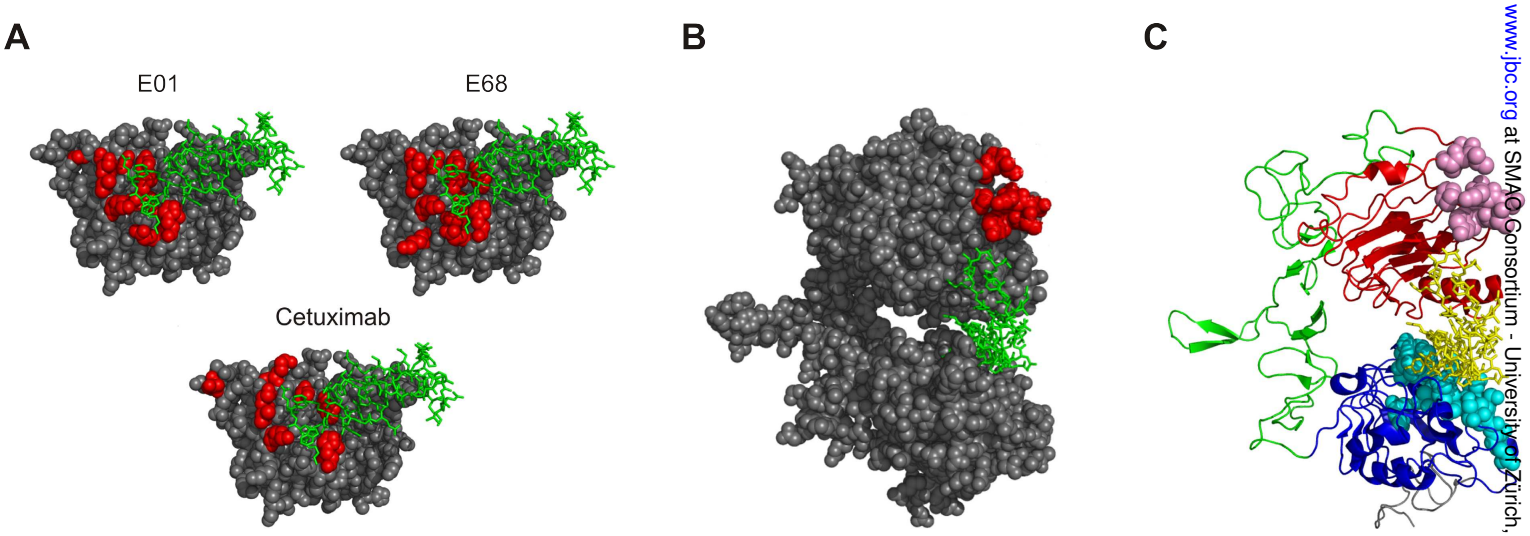

Figure 2

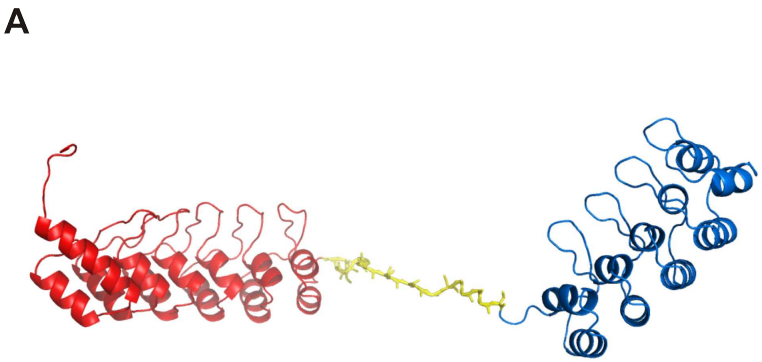

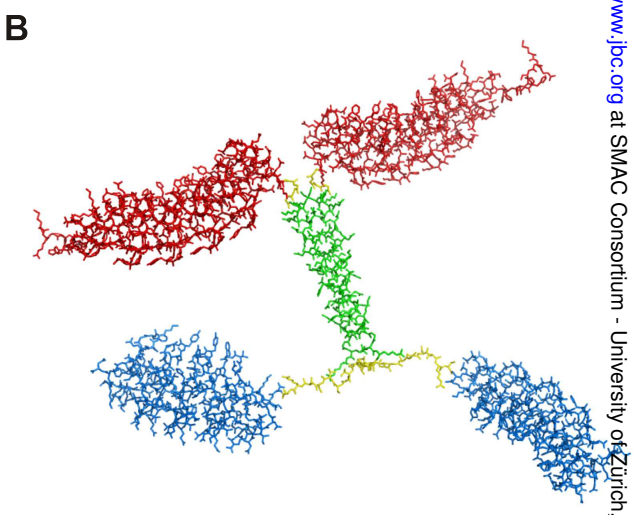

Figure 3

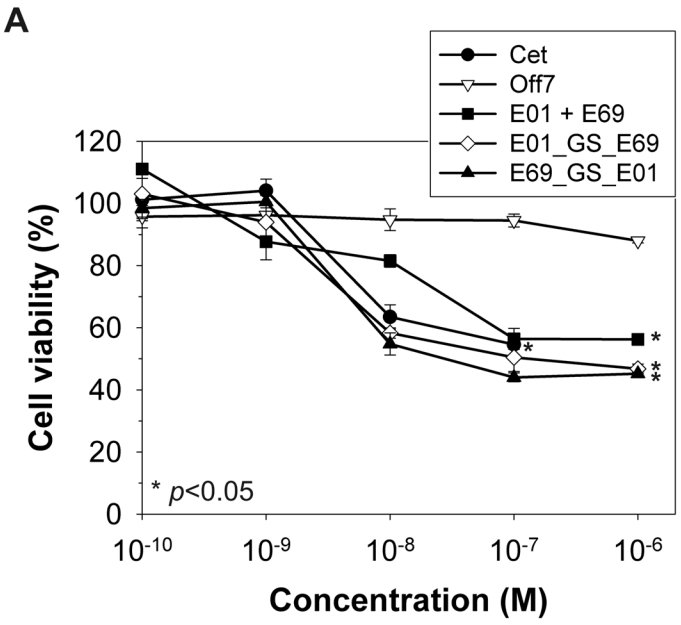

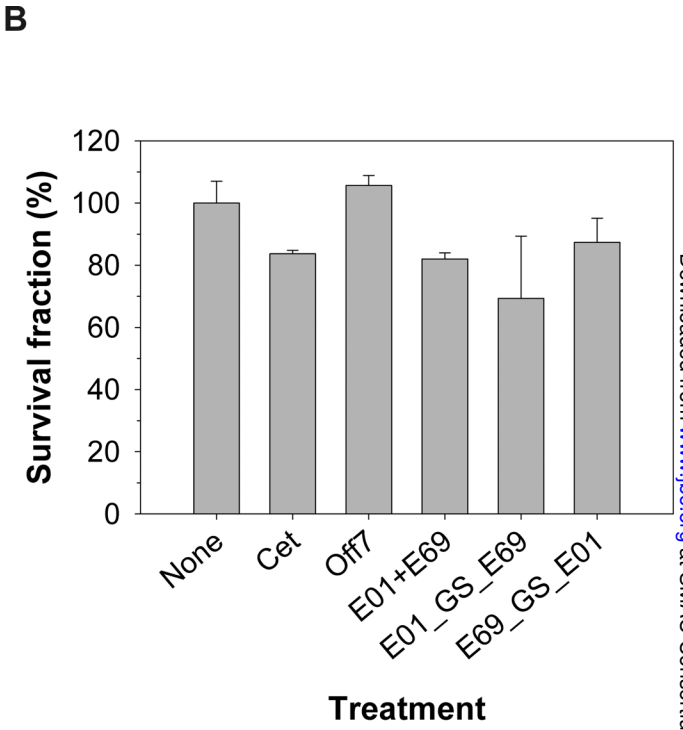

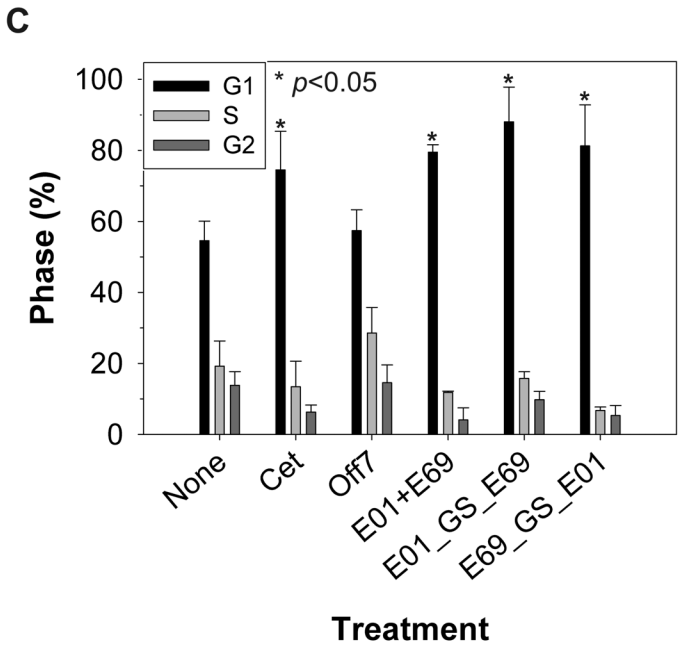

Figure 4

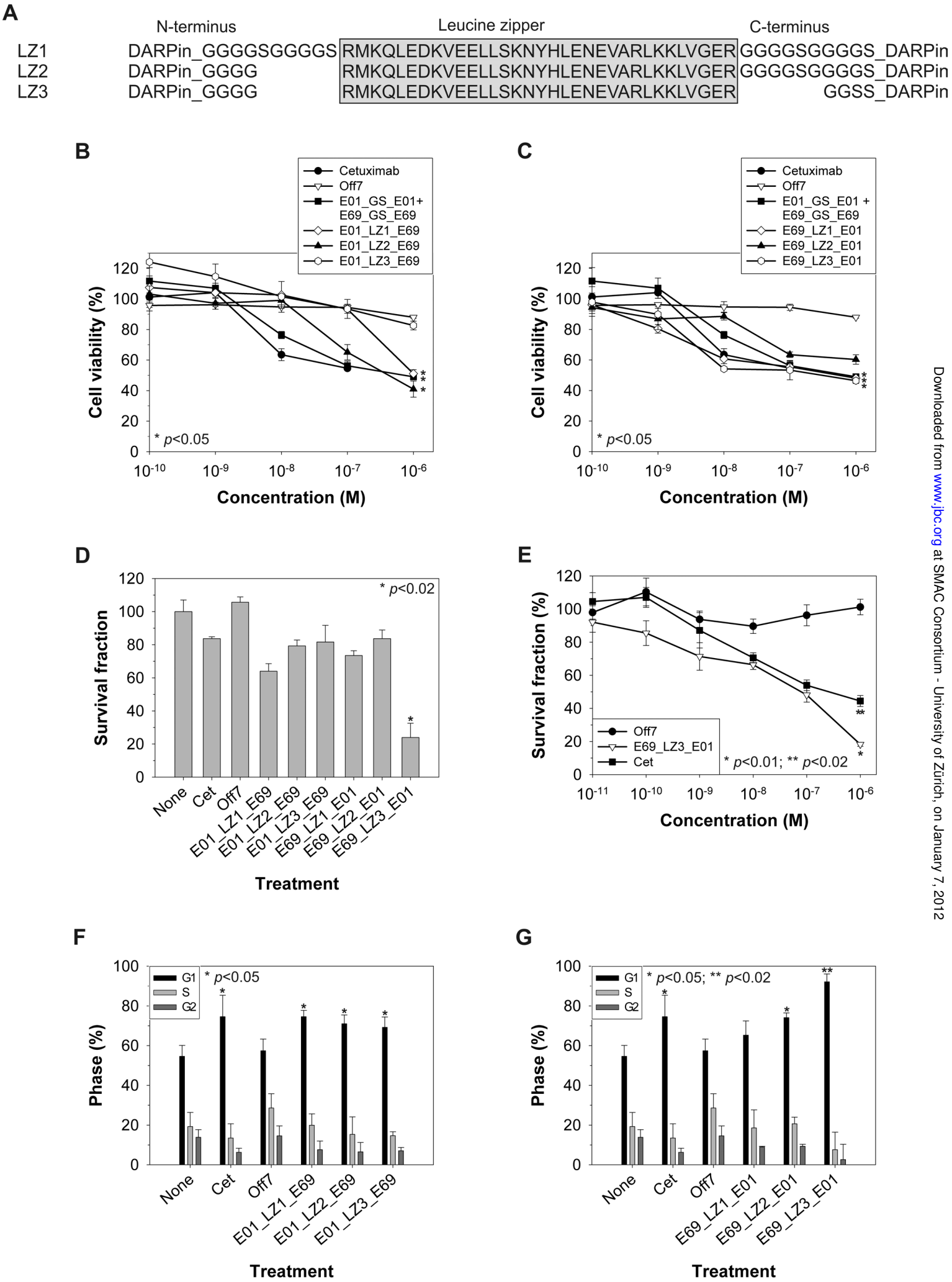

Figure 5

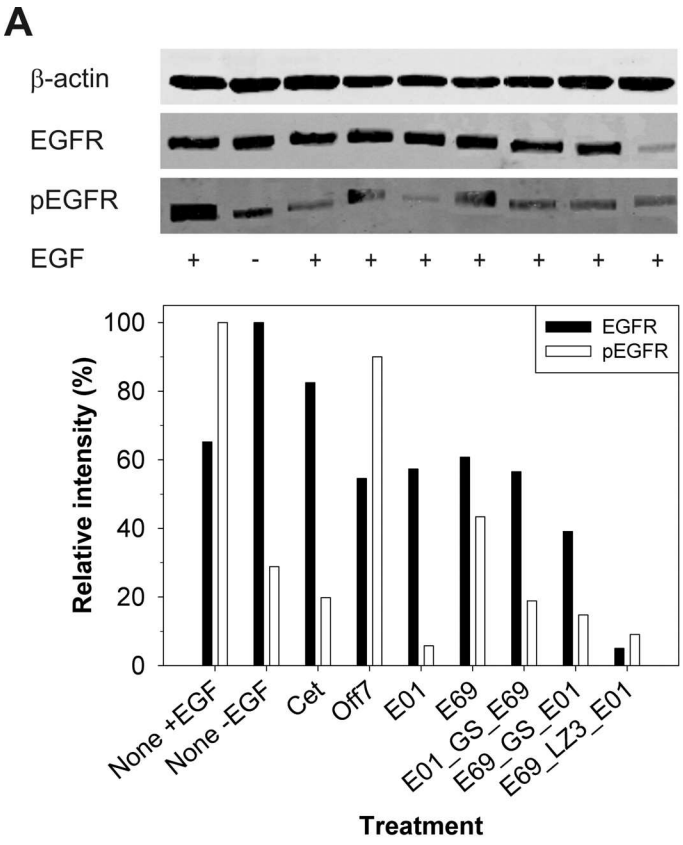

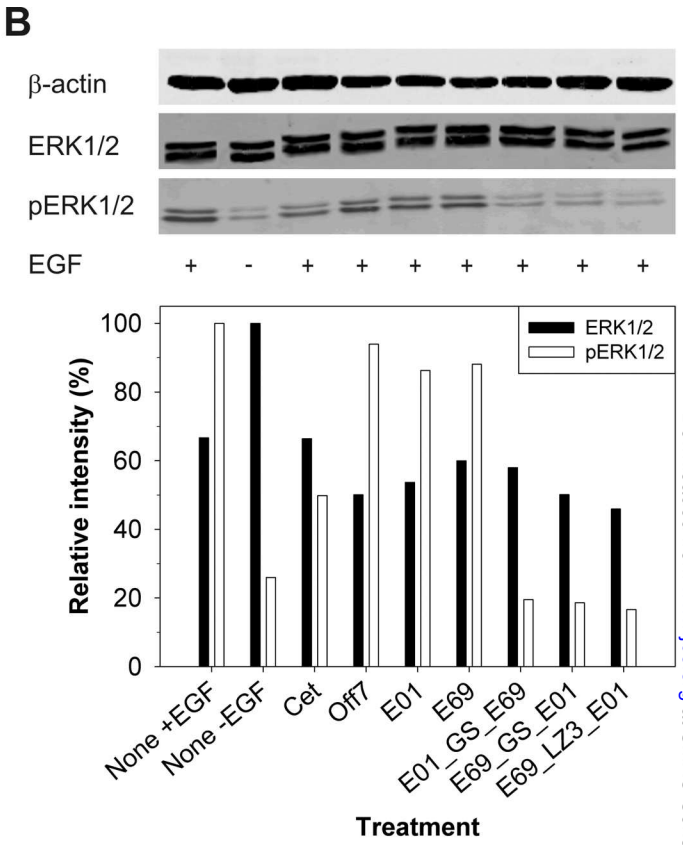

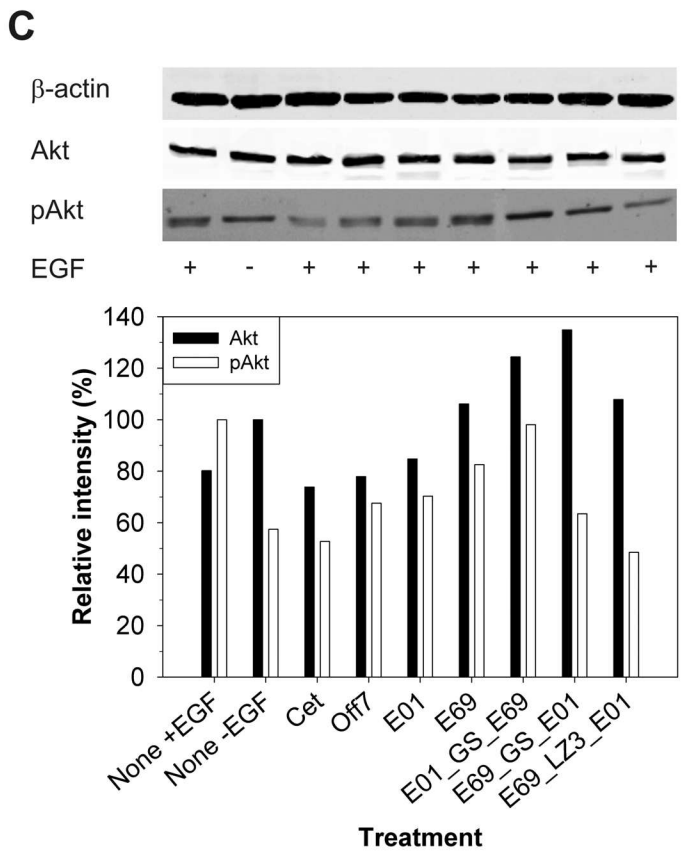

Figure 6

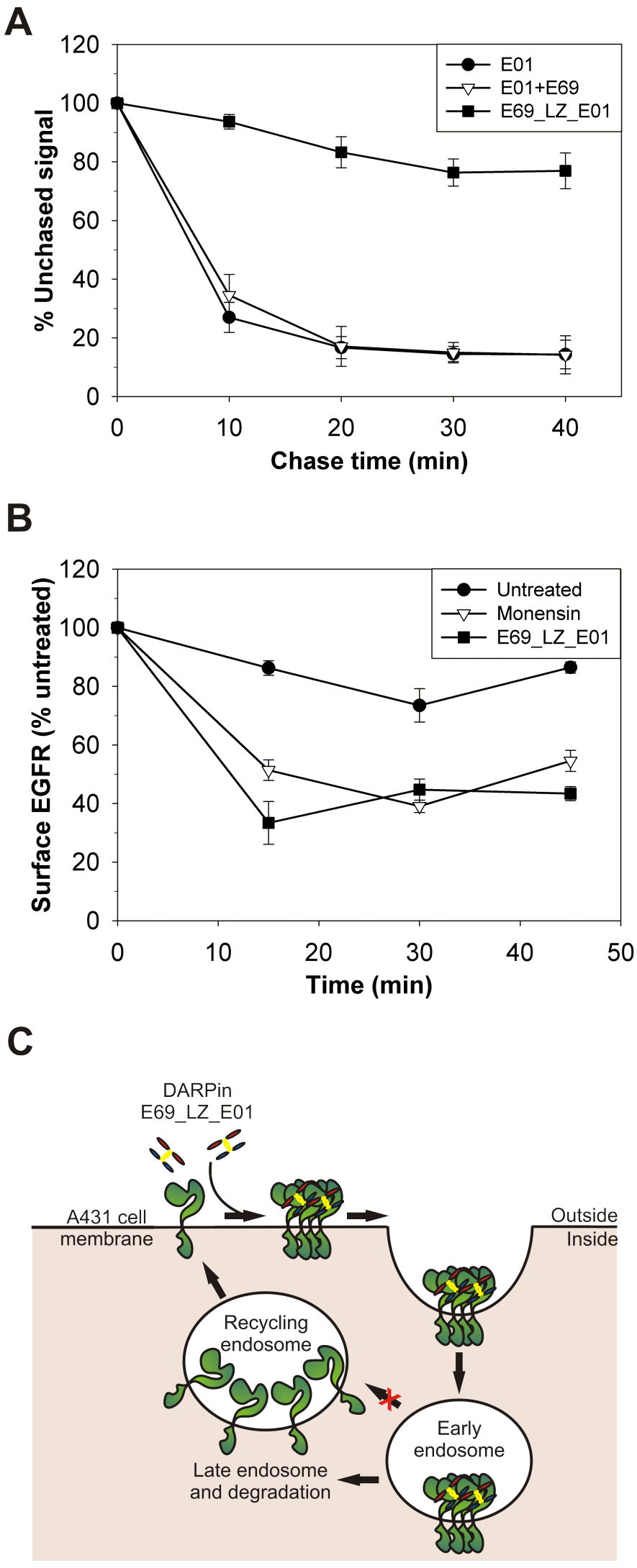

Fig. 7